JOURNAL OF CATALYSIS 38, 394–401 (1975)

Electron Spin Resonance Study of Supported Ruthenium Catalysts Promoted by Alkali Metal Salts in Dehydrogenation of Cyclohexane

M. KOBAYASHI AND T. SHIRASAKI

Tokyo Institute of Technology, Research Laboratory of Resources Utilization, O-okayama, Meguro-ku, Tokyo 152, Japan

Received October 30, 1974

The dehydrogenation of cyclohexane over Ru–silica and Ru–graphite catalysts promoted by alkali metal salts, was studied. Additions of KCN, LiCN and KCl enhanced the activity of the Ru–silica catalyst but NaCN, RbCN and CsCN had no effect. The activities for formation of benzene and cyclohexene over the Ru–silica catalysts had a maximum in the vicinity of K/Ru = 1 (atom ratio). On the other hand, CsCN, KCl, KCN and RbCN promoted the Ru–graphite catalyst but NaCN and LiCN had no effect. After the catalysts were reduced by H_2 at 500°C for 2 hr, about 50–80% of the KCN and KCl added to these catalysts, was not eluted from the catalysts with water. The ESR spectra of the Ru–silica catalysts which adsorbed cyclohexane and benzene at 500°C, were observed. There were three signals in these spectra of the catalysts promoted by KCN; a main singlet spectrum ($g = 2.009$) and two spectra of small intensity (splitting 58, 63 gauss). The splitting of the two signals for adsorbed cyclohexane was compatible with the results which were calculated for the coordination of cyclohexyl radicals to Ru (C_s symmetry) by Wolfsberg-Helmholz molecular orbital theory.

INTRODUCTION

The effect of promoter for supported ruthenium catalyst has been investigated by Urabe *et al.* (*1*), and they have concluded that the enhancement of activity in ammonia synthesis is caused by electron-donating of alkali metal to ruthenium. In their work, the evaporated alkali metal was used as promoter, but we adopted the impregnation method for addition of alkali metal salts. The first intention of the present investigation was to test the effect of promoters which were added as cyanide or chloride salts to ruthenium catalysts supported on silica and graphite in the dehydrogenation of cyclohexane, and the second was to survey the behavior of electrons which were shared between ruthenium and adsorbed hydrocarbons by the ESR spectra.

EXPERIMENTAL METHODS

The dehydrogenation of cyclohexane was performed with a usual differential flow reactor (*2*). Original catalysts were Ru–SiO_2–3O-2 and Ru-G-3 which had been reported in the preceding papers (*3,4*). Commercial potassium cyanide, potassium chloride and sodium cyanide were used for the preparation of the promoted catalysts, and lithium-, rubidium-, cesium-cyanide solutions were prepared from each chloride solution by anion exchange resin. We used mostly cyanide salts except for KCl in order to avoid the influence of different anion and alkali metal oxide. The original catalysts were impregnated in each cyanide or chloride solution with the desired concentration, and dried *in vacuo* at room temperature. The potassium contents of the catalysts were deter-

mined from analysis of the eluted solutions with water by atomic absorption spectroscopy (Jarrell-Ash AA-500). The other alkali metal contents were adjusted to alkali metal/Ru (atom ratio) = 1.

The apparatus and procedure for the samples of the ESR spectra were the same as that of the preceding paper (*4*). For the ESR spectra, only the catalysts supported on the silica gel were used, because any stable spectrum was not observed in the case of the graphite. The catalysts were reduced by H_2 gas flow at 500°C for 2 hr, and the evacuation was carried out below 1×10^{-4} Torr at 500°C for 2 hr. The thoroughly dehydrated and degassed cyclohexane or benzene vapor was allowed to stand in contact with these catalysts at 50–60 mm Hg, 500°C for 30 min, and the catalysts were evacuated at room temperature for 2 hr. The ESR spectra were observed at room temperature within 1 hr after the last evacuation under the following conditions; X band, time constant 1.0 sec, modulation amplitude 2.0 G, microwave power 50 MW, scan time 8 min, modulation frequency 100 kHz, microwave frequency 9.530–9.535 GHz (Varian E-12). Only the receiver gain was changed according to the intensity of signals. These spectra did not differ from those observed at −170°C.

RESULTS

Effect of the Promoters to Activity in Dehydrogenation of Cyclohexane

Preliminary experiments revealed that KCN and KCl did not promote the supported Ru catalysts in hydrogenation of benzene and that the amounts of adsorbed CO on these promoted catalysts were less than those of the original catalysts. Figure 1 illustrates the activity change of Ru–silica catalysts, with time, under constant conditions. It is clear that KCN, LiCN, and KCl promote Ru–silica catalyst but NaCN, RbCN, and CsCN have no effect.

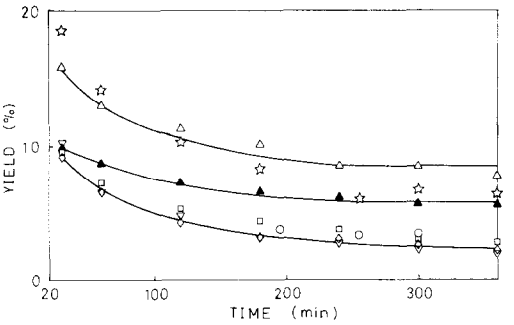

FIG. 1. Activity change with time: $t = 500$°C, $W/F_c = 6.04 \times 10^{-3}$, $W/F_t = 4.98 \times 10^{-4}$ [g min/ml(NTP)], $p_H = 0.189$ atm, (○) original catalyst $Ru-SiO_2$-30-2, (△) KCN, (☆) LiCN, (△) KCl, (□) NaCN, (◇) RbCN, (▽) CsCN.

The influence of potassium contents on activity was examined in the steady state. The results are shown in Figs. 2 and 3. With the benzene formation, the small values of cyclohexene yield also were plotted against K/Ru (atom ratio) in Fig. 2. The initial reaction rate constants were calculated from the following equations on the assumption that the promoter did not change the rate-determining step and the reaction mechanism; $r_1 = k_1 p_H^{-0.23} p_C^{1.1}$, $r_3 = k_3 p_H^{0.63} p_C^{0}$, ($r$: reaction rate; k: rate constant, suffix 1; 3: cyclohexene, benzene, respectively; p_H, p_C: partial pressure of H_2 and cyclohexane, respectively), which were determined according to the method of the preceding paper (*2*). The k_1 and k_3 were plotted against K/Ru in Fig. 3. The activities of the benzene and cyclohexene

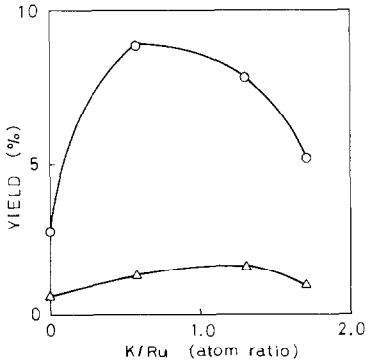

FIG. 2. Activity vs K/Ru: (○) benzene, (△) cyclohexene.

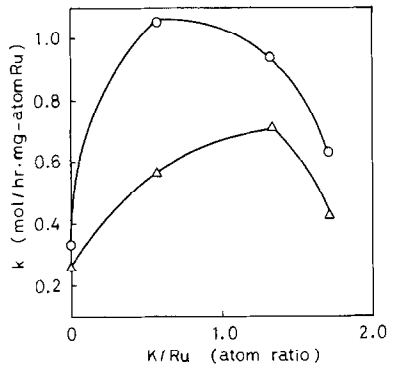

FIG. 3. Initial reaction rate constant vs K/Ru: (△) k_1 of cyclohexene formation, (○) k_3 of benzene formation.

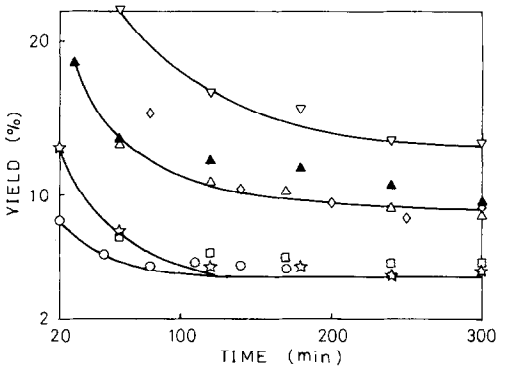

FIG. 4. Activity change with time: $t = 500°C$, $W/F_c = 4.51 \times 10^{-2}$, $W/F_t = 2.45 \times 10^{-3}$ [g min/ml(NTP)], $p_H = 0.377$ atm; (○) original catalyst Ru-G-3; (▽) CsCN, (▲) KCl, (◇) RbCN, (△) KCN, (□) NaCN, (☆) LiCN.

formation have a maximum in the vicinity of K/Ru = 1.

In the case of Ru–graphite catalyst, the effect of the promoters was examined much as in the Ru–silica catalyst. The results are shown in Fig. 4. It is the same tendency as the Ru–silica catalysts that KCN and KCl enhance the activity but NaCN does not. However, in contrast to the Ru–silica catalyst, CsCN and RbCN promote the Ru–graphite catalyst and LiCN does not except for the initial reaction time.

Next, we checked the affinity of KCN and KCl for these catalysts after reduction by H_2. The results are shown in Table 1. The left column of Table 1 was evaluated from the eluted solution of the catalysts which were not reduced, hence K/Ru means the potassium contents themselves. The right column shows the amounts of eluted potassium after reduction by H_2 at 500°C for 2 hr. The values of the right column are smaller than those of the left. This means that a large portion of the added KCN and KCl changed by reduction to the states which were not eluted with water.

TABLE 1
THE AMOUNTS OF POTASSIUM SALTS ELUTED FROM THE CATALYSTS WITH WATER

Catalyst	Without pretreatment		After reduction by H_2	
	K_2O[a] (mg-mol/g)	K/Ru (atom ratio)	K_2O[a] (mg-mol/g)	K/Ru (atom ratio)
Ru–SiO_2-30–KCN-A[b]	27.9 ($\times 10^{-3}$)	0.578	5.17 ($\times 10^{-3}$)	0.107
B[b]	63.0	1.302		
C[b]	82.6	1.710		
Ru–SiO_2-30-2–KCl	44.7	0.925	23.8	0.493
Ru-G-3–KCN	2.75	0.272	0.732	0.0725
Ru-G-3–KCl	16.2	1.604	2.93	0.290
SiO_2-30–KCN[c]	25.0		8.68	
G-KCN[c]	5.17		1.38	

[a] Converted values.
[b] Different contents were prepared.
[c] Ru is not contained.

ESR Spectra of Adsorbed Cyclohexane and Benzene on the Ru–Silica Catalysts

We could not observe ESR spectra of the original Ru–silica catalyst and the promoted Ru–silica catalysts which were not in contact with cyclohexane or benzene. The intensity of the ESR spectra decreased, when the adsorption of cyclohexane or benzene on these catalysts was performed at 400°C. The same temperature 500°C as the reaction condition was preferred for this study. The ESR spectra of adsorbed cyclohexene were also observed in the preliminary experiments, and these were similar to that of benzene. We took up only cyclohexane and benzene here.

After introduction of cyclohexane, the pressure increased slowly by about 10 mm Hg. It appears that dehydrogenation and cracking of cyclohexane occur. Figure 5 illustrates the ESR spectra of adsorbed cyclohexane on the various samples. There is a main spectrum of strong intensity ($g = 2.009$) on each sample, and the intensity of these spectra corresponds to the catalytic activity. Moreover, there are two signals of small intensity in the promoted catalysts ($g = 1.972$ and 2.044).

In contrast to cyclohexane, the pressure reduced gradually by about 10 mm Hg after benzene was introduced. The ESR spectrum of adsorbed benzene on the KCN-added Ru–silica catalyst was similar to that of cyclohexane, but there were no splitting spectra of small intensity (about 60 G) in the NaCN-added and original catalysts. The results are shown in Fig. 6.

Hydrogen gas (150–180 mm Hg) was introduced at room temperature for 30 min to the two samples which adsorbed cyclohexane or benzene at 500°C and were evacuated at room temperature for 1 hr. The ESR spectra were observed in the presence of hydrogen (20 mm Hg). The re-

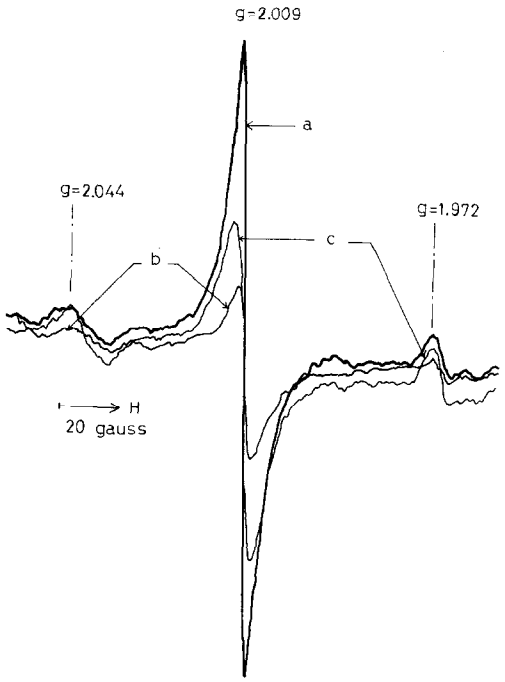

FIG. 5. ESR spectra of adsorbed C_6H_{12} on various samples: (a) KCN-added $Ru-SiO_2$-30-2; (b) $Ru-SiO_2$-30-2; (c) NaCN-added $Ru-SiO_2$-30-2; receiver gain 5.0×10^3.

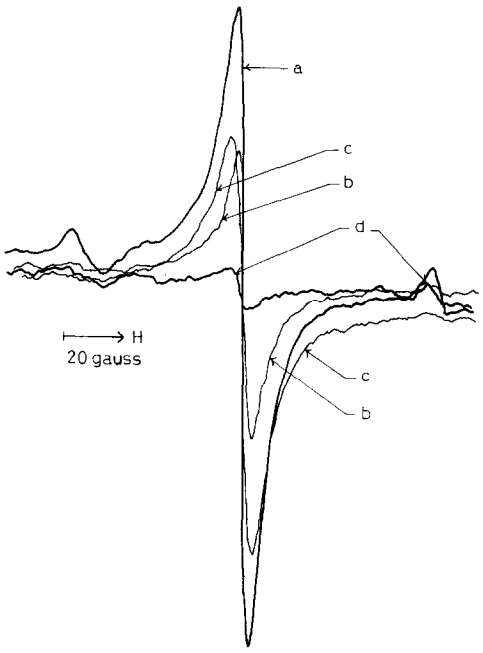

FIG. 6. ESR spectra of adsorbed C_6H_6 on various samples: (a,b,c) are the same as those of Fig. 5; (d) silica gel; receiver gain (a,c) 3.2×10^3, (b,d) 4.0×10^3.

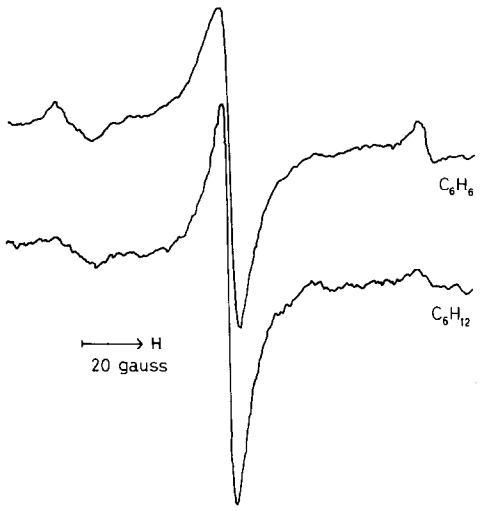

FIG. 7. ESR spectra of adsorbed C_6H_6 and C_6H_{12} on KCN-added Ru–SiO_2-30-2 affected by hydrogen: receiver gain, C_6H_6, 3.2×10^3; C_6H_{12}, 5.0×10^3.

sults are shown in Fig. 7. A main spectrum ($g = 2.009$) of each adsorbate became smaller by the influence of hydrogen. The splitting spectra of small intensity nearly diminished in the case of cyclohexane but remained unchanged in the case

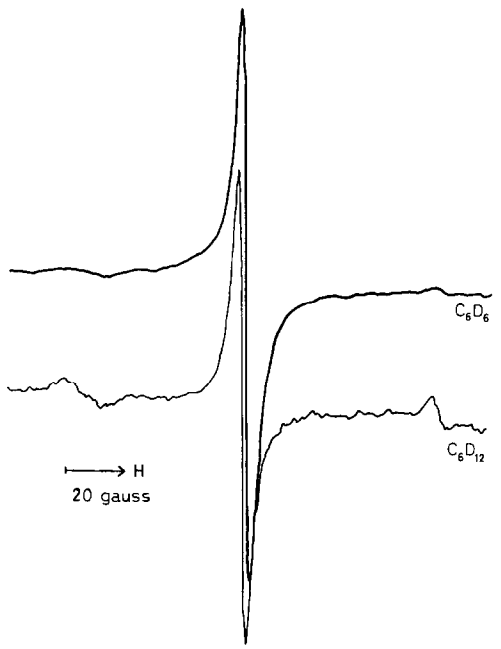

FIG. 8. ESR spectra of adsorbed C_6D_6 and C_6D_{12} on KCN-added Ru–SiO_2-30-2: receiver gain, C_6D_6, 1.60×10^3; C_6D_{12}, 5.0×10^3.

of benzene (compare Fig. 7 with (a) in Figs. 5 and 6).

Next we observed ESR spectra of adsorbed C_6D_{12} and C_6D_6 on the KCN-added Ru–silica catalysts. The results are shown in Fig. 8. A main spectral line became narrower, by using C_6D_{12} and C_6D_6. In C_6D_6 adsorbate, the splitting changed and diminished. On the contrary, the splitting lines of small intensity remained unchanged in C_6D_{12} adsorbate.

DISCUSSION

Assignment of the Signals in the ESR Spectra

As for the benzene adsorbate, the three signals of the ESR spectra observed in this study may be interpreted as due to the cyclohexadienyl ($C_6H_7\cdot$) and phenyl ($C_6H_5\cdot$) radicals (*5*) which are stabilized on the catalyst surface by carbonium ions or other radical species. These carbonium ions and radical species are partially reduced by hydrogen, and hence the intensity of a main signal ($g = 2.009$) decreases (Fig. 7). However, the splitting lines of small intensity remain unchanged because these are attributable to the partially anisotropic proton hyperfine coupling which is clear from the effect of C_6D_6 (Fig. 8). The splitting of about 60 G is close to 47.5 G of the irradiated solid benzene (*5*), and the difference may be responsible for the influence of ruthenium on these radicals. Examination of π-orbital in the benzene adsorbate by Wolfsberg–Helmholz theory was not performed because of the lack of overlap integral $S(2p_\pi, 4d_\pi)$ (*6*).

As for the cyclohexane adsorbate, a main spectrum may be assigned to unpaired electrons of various kinds of radicals but the splitting spectra of small intensity may not be interpreted as proton hyperfine coupling because of no difference with C_6D_{12} (Fig. 8). Here we tried an explanation of the splitting using Wolfsberg–Helmholz molecular orbital theory.

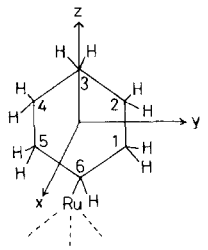

C_s	E	σ_h
A'	1	1
A''	1	-1

σ_h = xz-plane

FIG. 9. Model of cyclohexane adsorbed on ruthenium in C_s symmetry.

The C_s symmetry was considered as shown in Fig. 9 on the assumption that the bond structures between Ru atoms (broken line in Fig. 9) can be neglected and that the adjacent Ru atoms change only the ionization potentials of the Ru atom bonded to the cyclohexyl radical. From extended Hückel theory, the following ligand orbitals were derived for each irreducible representation A' and A''.

$$\varphi_1(A') = (1/\sqrt{2})(1s_1 + 1s_5),$$
$$\varphi_1'(A') = (1/\sqrt{2})(1s_1' + 1s_5'),$$
$$\varphi_2(A') = (1/\sqrt{2})(1s_2 + 1s_4),$$
$$\varphi_2'(A') = (1/\sqrt{2})(1s_2' + 1s_4'),$$
$$\varphi_3(A') = 1s_3,$$
$$\varphi_3'(A') = 1s_3',$$
$$\varphi_4(A') = 1s_6,$$
$$\phi_1(A') = (1/\sqrt{2})(2s_1 + 2s_5),$$
$$\phi_2(A') = (1/\sqrt{2})(2s_2 + 2s_4),$$
$$\phi_3(A') = 2s_3,$$
$$\phi_4(A') = 2s_6,$$
$$\psi_1(A') = (1/\sqrt{2})(2p_{x1} + 2p_{x5}),$$
$$\psi_2(A') = (1/\sqrt{2})(2p_{y1} - 2p_{y5}),$$
$$\psi_3(A') = (1/\sqrt{2})(2p_{z1} + 2p_{z5}),$$
$$\psi_4(A') = (1/\sqrt{2})(2p_{x2} + 2p_{x4}),$$
$$\psi_5(A') = (1/\sqrt{2})(2p_{y2} - 2p_{y4}),$$
$$\psi_6(A') = (1/\sqrt{2})(2p_{z2} - 2p_{z4}),$$
$$\psi_7(A') = 2p_{x3},$$
$$\psi_8(A') = 2p_{z3},$$
$$\psi_9(A') = 2p_{x6},$$
$$\psi_{10}(A') = 2p_{z6},$$
$$\varphi_1(A'') = (1/\sqrt{2})(1s_1 - 1s_5),$$
$$\varphi_1'(A'') = (1/\sqrt{2})(1s_1' - 1s_5'),$$
$$\varphi_2(A'') = (1/\sqrt{2})(1s_2 - 1s_4),$$
$$\varphi_2'(A'') = (1/\sqrt{2})(1s_2' - 1s_4'),$$
$$\phi_1(A'') = (1/\sqrt{2})(2s_1 - 2s_5),$$
$$\phi_2(A'') = (1/\sqrt{2})(2s_2 - 2s_4),$$
$$\psi_1(A'') = (1/\sqrt{2})(2p_{x1} - 2p_{x5}),$$
$$\psi_2(A'') = (1/\sqrt{2})(2p_{y1} + 2p_{y5}),$$
$$\psi_3(A'') = (1/\sqrt{2})(2p_{z1} - 2p_{z5}),$$
$$\psi_4(A'') = (1/\sqrt{2})(2p_{x2} - 2p_{x4}),$$
$$\psi_5(A'') = (1/\sqrt{2})(2p_{y2} + 2p_{y4}),$$
$$\psi_6(A'') = (1/\sqrt{2})(2p_{z2} - 2p_{z4}),$$
$$\psi_7(A'') = 2p_{y3},$$
$$\psi_8(A'') = 2p_{y6},$$

The sets of molecular orbitals are shown in Table 2. Electron configuration of the Ru atoms is taken as Ru^0, $[Kr](4d)^7(5s)^1$ or Ru^+, $[Kr]\ (4d)^7$ in which the valence electrons are $5s$ and $4d_{z^2}$ in the atomic orbitals, and then the residual six electrons occupying $4d_{xy}$, $4d_{yz}$, $4d_{xz}$, form a closed shell and have no paramagnetism. Consequently, the irreducible representation of σ-bondings is C_s (A'), and the ligand orbitals ϕ_4, ψ_{10} which consist of $2s$ and $2p_z$ orbitals of the sixth carbon atom, form the molecular orbitals mixing with $5s$ and $4d_{z^2}$ of the Ru atom. The results were:

$$\Psi_1(A') = a(4d_{z^2}) + b\psi_{10},$$
$$\Psi_2(A') = a(5s) + b\psi_{10},$$
$$\Psi_3(A') = a(4d_{z^2}) + b\phi_4,$$
$$\Psi_4(A') = a(5s) + b\phi_4, \qquad (1)$$

here, a and b are the weighting (mixing) coefficients. The Zeeman terms become:

$$\langle\Psi_n(A')\alpha|L_z + 2S_z|\Psi_n(A')\alpha\rangle = a^2 + b^2,$$
$$\langle\Psi_n(A')\beta|L_z + 2S_z|\Psi_n(A')\beta\rangle = -a^2 - b^2,$$
$$\langle\Psi_n(A')\alpha|L_x + 2S_x|\Psi_n(A')\beta\rangle = a^2 + b^2,$$
$$\langle\Psi_n(A')\beta|L_x + 2S_x|\Psi_n(A')\alpha\rangle = -a^2 - b^2,$$
$$(n = 1, 2, 3, 4),$$

then, the g-values become:

$$g_{\|} = g_{\perp} = 2(a^2 + b^2). \qquad (2)$$

TABLE 2
ORBITAL SCHEME IN C_s SYMMETRY

Representation	Ru orbitals	Ligand orbitals
A'	$5s$, $4d_{z^2}$, $4d_{xy}$	φ_1, φ_2, φ_1', φ_2', ϕ_{1-4}, ψ_{1-10}
A''	$4d_{yz}$, $4d_{xz}$	φ_1, φ_2, φ_1', φ_2', ϕ_1, ϕ_2, ψ_{1-8}

The energies may be obtained by solving the secular determinants:

$$|H_{ij} - G_{ij}E| = 0,$$

for each $\Psi_n(A')$. Here, H_{ij} were approximated by the following relation:

$$H_{ij} = FG_{ij}(H_{ii} + H_{jj})/2,$$

where, F is 1.7 for the σ-bonding according to Wolfsberg–Helmholz, and H_{ii}, H_{jj} are the ionization potentials of the metal atom and its ligand, respectively. The values of H_{ii} for Ru^0 and Ru^+ are -7.364 and -16.76 eV, respectively (*7*). We adopted the ionization potential of cyclohexane -10.50 eV (*8*) for H_{jj} tentatively though it is desirable to use the ionization potential of cyclohexyl radical for each electronic structure. The group overlap integrals G_{ij} in these orbitals are equal to the atomic overlap integrals S_{ij}: $S(2p_\sigma, 4d_\sigma)$, $S(2p_\sigma, 5s)$, $S(2s, 4d_\sigma)$, $S(2s, 5s)$. The values of S_{ij} were cited from the reports of Clementi *et al.* (*9*), Jaffé (*10*) and Leifer *et al* (*6*). The value of R for calculation of the parameters was assumed to be 2.10 Å according to Pauling's study. Calculation of the weighting (mixing) coefficients a and b are allowed by substitution of the molecular orbital energies into the secular equation:

$$a(H_{ii} - E) + b(H_{ij} - G_{ij}E) = 0,$$

and using the normalization condition:

$$a^2 + 2abG_{ij} + b^2 = 1$$

The results are shown in Table 3. Next, we must select the one bonding-orbital and the one antibonding-orbital for the configuration of the unpaired electron. The 2*s* orbital of the sixth carbon atom is used in bonding with adjacent the sixth hydrogen atom, the first and the fifth carbon atoms by hybridization (Fig. 9), and hence the only $\Psi_1(A')$ and $\Psi_2(A')$ in Eq. (1) are possible. As shown in Table 3, $\Psi_1{}^b$ and $\Psi_3{}^b$ have the same energy level so that they are degenerate and may be more stabilized by

TABLE 3
GROUP OVERLAP INTEGRALS AND MOLECULAR ORBITAL ENERGIES

		Bonding levels			Antibonding levels		
	G	$-E$ (eV)	a	b	$-E$ (eV)	a^*	b^*
Ru^0							
$\Psi_1(A')$	0.0845	10.543	0.121	0.980	7.228	0.965	−0.195
$\Psi_2(A')$	0.241	10.817	0.274	0.899	6.274	0.993	−0.504
$\Psi_3(A')$	0.051	10.532	0.0743	0.993	7.307	1.00	−0.142
$\Psi_4(A')$	0.325	11.015	0.316	0.850	5.379	1.009	−0.628
Ru^+							
$\Psi_1(A')$	0.0845	16.80	0.992	0.0736	10.32	0.169	−1.000
$\Psi_2(A')$	0.241	17.90	0.928	0.209	9.00	0.445	−1.010
$\Psi_3(A')$	0.051	16.80	0.989	0.1602	10.43	0.1027	−1.000
$\Psi_4(A')$	0.325	17.30	0.890	0.252	7.71	0.570	−1.028

the configuration-interaction of electrons. When electrons are in excess in ruthenium or cyclohexane, $\Psi_2{}^b$ is filled with a pair of electrons and an unpaired electron occupies the antibonding orbital of the lowest level $\Psi_1{}^*$, or an electron hole in $\Psi_1{}^*$ should be treated as a magnetic electron. The several models of the unpaired electron-configuration are shown in Fig. 10 with the corresponding g-values (g_{calc}) which are calculated from Eq. (2) and Table 3. Here an open dot means an electron hole. The g-values (g_{calc}) are close to the experimental values (g_{obs}), and the two

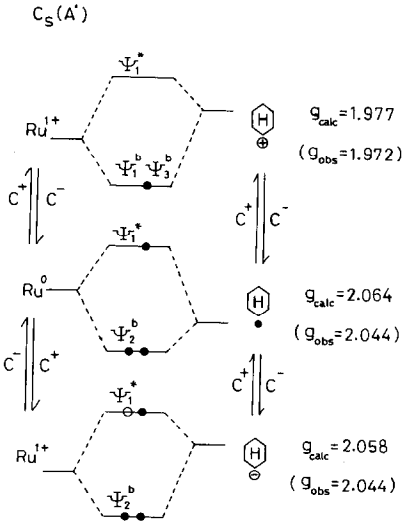

FIG. 10. Molecular orbital diagram for cyclohexane adsorbed on ruthenium and resonance stabilization with carbonium ions.

different ionization potentials of ruthenium have no serious effect upon the g-values. The difference between the g_{calc} and g_{obs} may be caused by the uncertainty of the ionization potential for cyclohexyl radical. The results for another symmetry C_{2v} did not agree with the experimental data.

Effect of the Promoters and the ESR Spectra

It was well confirmed from the result of Table 1 that KCN and KCl combine with the Ru metal and the catalyst supports. It can be seen from Figs. 1 and 4, that the working of the promoter is influenced by the catalyst support, and that there are characteristics for each alkali metal salt. From the results of the preliminary experiments described above, it is likely that KCN and KCl are effective only for the dehydrogenation and that the enhancement of activity is not attributable to the change of physical properties, e.g., surface area.

As for cyclohexane, the correspondence between the ESR spectra and the activity may be explained as follows. From the increasing of pressure described above, a main spectrum of $g = 2.009$ is attributable not only to cyclohexyl and phenyl radicals but also to various carbonium ions which are produced by the dehydrogenation as much as to be active, and hence the intensity of spectrum decreases by hydrogen adsorption (Fig. 7). It can therefore be presumed that the promoter KCN stabilizes these carbonium ions and that these ions induce ionization of ruthenium and cyclohexane, that is, the resonance stabilization takes place as is shown in Fig. 10, where C^+ and C^- mean radical species, e.g., carbonium cation and anion, respectively. The dehydrogenation of cyclohexane seems to proceed partially stepwise, and hence it is natural that the partially dehydrogenated adsorbate exists as shown in Fig. 9. Consequently, the KCN-added catalyst, which shows the splitting spectra, has the effective ability for cyclohexene formation (Fig. 2). In the case of cyclohexane dehydrogenation on Pd–alumina and Pt–alumina catalysts, Maatman *et al.* (*11*) have recently shown that the reaction proceeds via a mechanism whose slow step is a monomolecular decomposition of reactant on the catalyst surface, and that cyclohexene is a necessary intermediate. The consideration described above is to some extent substantiated by the results of Maatman *et al.* in spite of the different catalysts and reaction conditions.

As for benzene, it seems likely that KCN excites the interaction between carbonium ions and π-electrons of benzene and cyclohexene, and that KCN induces the polarization of spin dipole moment by the $\sigma-\pi$ interaction. Through these actions, the products, viz, benzene and cyclohexene may be stabilized.

ACKNOWLEDGMENTS

The authors thank Mr. Y. Nakamura (Tokyo Institute of Technology, Research Laboratory of Resources Utilization) for his measurement of the ESR spectra and Mizusawa Kagaku Kogyo Co., Ltd., for the analysis of the alkali metals.

REFERENCES

1. Urabe, K., Aika, K., and Ozaki, A., *J. Catal.* **32,** 108 (1974).
2. Kobayashi, M., Fukuda, S., and Shirasaki, T., *Nippon Kagaku Kaishi 1973,* 464 (3).
3. Kobayashi, M., and Shirasaki, T., *J. Catal.* **28,** 289 (1973).
4. Kobayashi, M., and Shirasaki, T., *J. Catal.* **32,** 254 (1974).
5. Ohnishi, S., Tanei, T., and Nitta, I., *J. Chem. Phys.* **37,** 2402 (1962).
6. Leifer, L., Cotton, F. A., and Leto, J. R., *J. Chem. Phys.* **28,** 364 (1958).
7. Moore, C. E., "Atomic Energy Levels," Vol. 3. Nat. Bur. Stand. (U.S.), Washington, DC, 1958.
8. Pottie, R. F., Harrison, A. G., and Lossing, F. P., *J. Amer. Chem. Soc.* **83,** 3204 (1961).
9. Clementi, E., Raimondi, D. L., and Reinhardt, W. P., *J. Chem. Phys.* **47,** 1300 (1967).
10. Jaffé, H. H., *J. Chem. Phys.* **21,** 258 (1953).
11. Maatman, R., Ribbens, W., and Vonk, B., *J. Catal.* **31,** 384 (1973).